

# Dehydrocyclooctatetraene. Photoelectron Spectroscopy of the $C_8H_6^-$ Anion

Paul G. Wenthold<sup>\*,†</sup> and W. C. Lineberger<sup>\*</sup>

Contribution from JILA, University of Colorado, Boulder, Colorado 80309-0440, and National Institute of Standards and Technology and Department of Chemistry and Biochemistry, University of Colorado, Boulder, Colorado 80309-0440

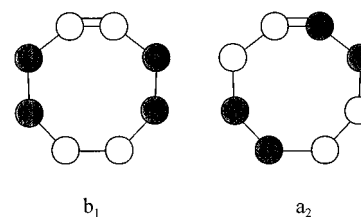
Received March 24, 1997<sup>⊗</sup>

**Abstract:** The photoelectron spectrum of the dehydrocyclooctatetraene negative ion,  $C_8H_6^-$ , is reported. The spectrum strongly resembles that previously reported for the cyclooctatetraene anion, indicating that the structure of  $C_8H_6^-$  is very similar to that of  $C_8H_8^-$ . Two electronic states of dehydrocyclooctatetraene are observed in the photoelectron spectrum. The lowest energy feature is assigned to singlet 1,3,5-cyclooctatrien-7-yne, while the higher energy band corresponds to a triplet state of dehydrocyclooctatetraene. The electron affinity of  $C_8H_6$  is found to be  $1.044 \pm 0.008$  eV, and the energy difference between the singlet and triplet states is  $0.708 \pm 0.006$  eV. Vibrational activity is observed in the photoelectron spectrum and assigned using a simple potential energy surface. Stretching of the triple bond in cyclooctatrienyne is found to have a frequency of  $2185\text{ cm}^{-1}$ , essentially what is expected for a triple bond within an eight-membered ring. *Ab initio* and density functional molecular orbital calculations on dehydrocyclooctatetraene and the corresponding ions are reported. Cyclooctatrienyne is calculated to have a planar or pseudoplanar structure, consistent with assignments based on peak widths in the photoelectron spectrum.

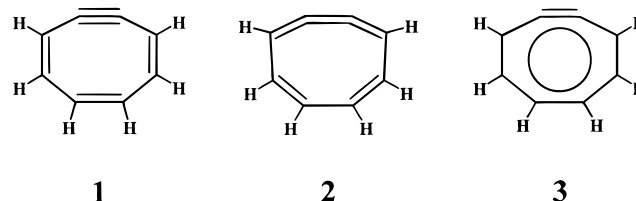
A continuing challenge for chemists is the preparation and characterization of cyclic molecules that contain a triple bond. Although they are typically highly strained, many cyclic alkynes have been prepared and characterized.<sup>1</sup> Cyclooctyne is the smallest unsubstituted cycloalkyne that can be isolated,<sup>2,3</sup> but spectroscopic evidence for systems as small as cyclopentyne has been provided.<sup>4</sup> In many cases, the sole evidence for the existence of the intermediate is the products obtained in cycloaddition reactions with diene trapping reagents.

In this paper, we report our studies of dehydrocyclooctatetraene (DHCOT), a cyclic alkyne that has been trapped in this fashion. Many previous studies have been carried out on DHCOT, studies primarily designed to investigate the extent of planarity in the molecule. Semiempirical MO calculations have been used to investigate the possible electronic states of DHCOT. Using MINDO/3, Huang *et al.*<sup>5</sup> found that introducing a triple bond into cyclooctatetraene (COT) to form 1,3,5-cyclooctatrien-7-yne, **1**, leads to planarization of the normally tub-shaped molecule.<sup>6</sup> The highest occupied (HOMO) and lowest unoccupied (LUMO) molecular orbitals of **1** are shown in Chart 1. The HOMO is a bonding  $b_1$   $\pi$  orbital, and is similar to the  $b_{1u}$  orbital in planar COT.<sup>7,8</sup> The LUMO of **1** is an antibonding  $a_2$  orbital, and resembles the  $b_{2u}$  orbital in planar COT. From these orbitals, it is possible to form additional electronic states of DHCOT. For example, double occupancy

Chart 1



of the  $a_2$  orbital gives 1,2,3,5,7-cyclooctapentaene, **2**, which has a cyclic cumulene structure. Calculations on **1**, **2**, and additional DHCOT isomers were carried out by using MNDO<sup>9</sup> and MNDO/CI<sup>10</sup> protocols. In all cases, **1** was found to be the lowest energy monocyclic state, with **2** higher in energy by 9 to 57 kcal/mol.<sup>9,10</sup> A  $^3B_2$  state of DHCOT, **3**, is formed by single occupation of each orbital. There have not been any previous studies of this electronic state.



Experimental evidence for the existence of **1** is inferred from studies of reaction products and mechanisms. Krebs<sup>11</sup> has shown that the reaction of bromocyclooctatetraene with potassium *tert*-butoxide in the presence of tetraphenylcyclopentadienone or phenyl azide leads to the formation of cyclooctatetraene derivatives as shown in eqs 1 and 2, respectively. If the reaction is carried out without the trapping agents, the products shown in eq 3 are obtained. These results indicate the presence of

<sup>†</sup> Present address: Department of Chemistry and Biochemistry, Texas Tech University, Lubbock, TX 79409-1061.

(1) Krebs, A.; Wilke, J. *Top. Curr. Chem.* **1983**, *109*, 189 and references therein.

(2) Blomquist, A. T.; Liu, L. H. *J. Am. Chem. Soc.* **1953**, *75*, 2153.

(3) Wittig, G.; Krebs, A. *Chem. Ber.* **1961**, *94*, 3260.

(4) Chapman, O. L.; Gano, J.; West, P. R.; Regitz, M.; Maas, G. *J. Am. Chem. Soc.* **1981**, *103*, 7033.

(5) Huang, N. Z.; Mak, T. C. W.; Li, W.-K. *Tetrahedron Lett.* **1981**, *38*, 3765.

(6) Bastiansen, O.; Hedberg, L.; Hedberg, K. *J. Chem. Phys.* **1957**, *27*, 1311.

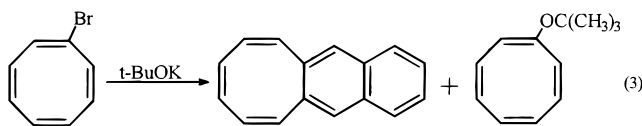
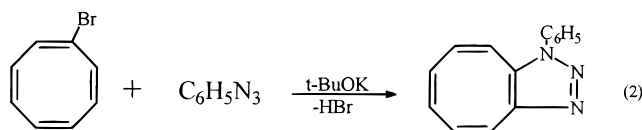
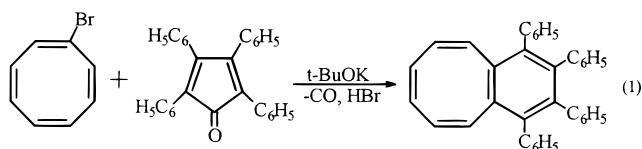
(7) Hrovat, D. A.; Borden, W. T. *J. Am. Chem. Soc.* **1992**, *114*, 5879.

(8) Wenthold, P. G.; Hrovat, D.; Borden, W. T.; Lineberger, W. C. *Science* **1996**, *272*, 1456.

(9) Glidewell, C.; Lloyd, D. *Tetrahedron* **1984**, *40*, 4455.

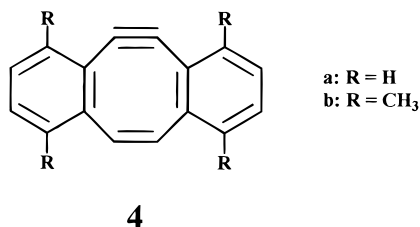
(10) Dewar, M. J. S.; Merz, K. M., Jr. *J. Am. Chem. Soc.* **1985**, *107*, 6175.

(11) Krebs, A. *Angew. Chem., Int. Ed. Engl.* **1965**, *4*, 953.



cyclooctatrienyne, **1**. Products corresponding to trapping of **2** were not reported for these reactions,<sup>11,12</sup> which suggests that **2** either does not exist or is much higher in energy than **1**. Additional instances of the trapping of **1** have subsequently been reported.<sup>13–17</sup>

Although **1** itself is too reactive to be isolated, stable annulated derivatives, such as **4**, have been prepared and characterized.<sup>18–21</sup> These derivatives are essentially planar, with large CCC bond angles about the acetylenic carbons. The bond lengths between the dehydrocarbons were found by using X-ray crystallography to be  $1.211 \pm 0.008$  and  $1.22 \pm 0.010$  Å for **4a**<sup>20</sup> and **4b**,<sup>21</sup> respectively, indicating a high degree of triple bond character.



Upon cursory inspection, planar **1** would appear to resemble its 6-member-ring counterpart, *o*-benzyne. Both molecules are planar and fully conjugated. However, while the  $\pi$  system of *o*-benzyne is aromatic and delocalized,<sup>22</sup> **1** is not aromatic, and it has alternating single and double bonds.<sup>9,10</sup> We have now used negative ion photoelectron spectroscopy to study the properties of DHCOT. We have found that the lowest energy form of the DHCOT ion consists of attachment of an electron to **1**, and, upon detachment of the ion, both **1** and **3** are formed. The photoelectron spectrum of the negative ion of DHCOT, **1**<sup>-</sup>, is significantly different than that of the *o*-benzyne ion<sup>23</sup> and, rather, is very similar to the photoelectron spectrum of the

cyclooctatetraene negative ion, COT<sup>-</sup>.<sup>8</sup> The C≡C stretching frequency in **1** is found to be  $2185 \text{ cm}^{-1}$ , much higher than that in *o*-benzyne but consistent with what is expected for a normal triple bond. Finally, the singlet–triplet splitting in DHCOT is obtained, and found to be comparable to that in planar COT.

## Experimental Section

The photoelectron spectrometer and experimental procedures used to carry out this work have been described in detail previously,<sup>24</sup> and only a summary is provided here. Atomic oxygen ions, O<sup>-</sup>, are created by a microwave discharge in O<sub>2</sub> seeded in approximately 0.5 Torr of helium in a liquid nitrogen cooled flowing afterglow apparatus. Cyclooctatetraene is added through ring inlets downstream from the discharge source. The O<sup>-</sup> ion abstracts H<sub>2</sub><sup>+</sup> from COT to make C<sub>8</sub>H<sub>6</sub><sup>-</sup> ions.<sup>25</sup> A small portion of the ions in the flowing afterglow are extracted through a 1-mm orifice in a nosecone into a differentially pumped chamber, where they are focused, accelerated to 735 eV, mass selected by using a Wien velocity filter ( $M/\Delta M \approx 40$ ), and decelerated to 40 eV. The ion beam is crossed with the 351-nm output of an argon ion laser in a build-up cavity described in detail previously.<sup>24</sup> Photodetached electrons are energy analyzed by using a hemispherical analyzer, which has a resolution of *ca.* 8 meV, and detected using position-sensitive detection. The photoelectron spectrum depicts the number of electrons detected as a function of electron binding energy, the difference between the laser photon energy (3.531 19 eV) and the electron kinetic energy.

The absolute energy scale is calibrated by using the position of the  $^3P_2 + e^- \leftarrow ^2P_{3/2}$  peak in the spectrum of O<sup>-</sup> (EA(O) = 1.461 12 eV).<sup>26</sup> A small energy scale compression factor is determined by comparing the measured relative peak positions in the spectrum of tungsten ion with the known term energies of the tungsten atom.<sup>27</sup> The extent of the scale compression is less than 1%, and absolute photoelectron energies can be obtained to an accuracy of  $\pm 0.003$  meV.

**Materials.** All reagents were purchased from commercial suppliers and were used as received. Cyclooctatetraene (98%) was obtained from Aldrich. Gas purities were He (99.995%) and O<sub>2</sub> (99%).

## Results and Discussion

In this section, we present the photoelectron spectrum of the DHCOT anion, **1**<sup>-</sup>, along with a vibrational analysis. However, before doing so, we provide a description of the structure of the electronic states of DHCOT and the negative ions derived from them. An understanding of the electronic structure is essential in order to interpret the photoelectron spectrum.

**Electronic Structure Calculations.** We have used *ab initio* and density functional calculations to investigate the geometries and energies of planar **1**, **2**, and **3**.<sup>28</sup> The geometries calculated at the Becke3LYP/6-31G\* and R(O)HF/6-31G\* levels of theory are shown in Figure 1. As expected, **1** and **2** clearly contain alternating single and double bonds, while the bond lengths calculated for **3** are essentially midway between those in **1** and **2**. The bond angles do not differ significantly among the three

(12) Krebs, A.; Byrd, D. *Liebigs Ann. Chem.* **1967**, 707, 66.

(13) Sanders, D. C.; Marczak, A.; Melendez, J. L.; Schechter, H. *J. Org. Chem.* **1987**, 52, 5622.

(14) Harmon, C. A.; Streitwieser, A., Jr. *J. Org. Chem.* **1973**, 38, 549.

(15) Lankey, A. S.; Ogliauso, M. A. *J. Org. Chem.* **1971**, 36, 3339.

(16) Elix, J. A.; Sargent, M. V.; Sondheimer, F. *J. Am. Chem. Soc.* **1970**, 92, 963.

(17) Elix, J. A.; Sargent, M. V. *J. Am. Chem. Soc.* **1969**, 91, 4734.

(18) Wong, H. N. C.; Garratt, P. J.; Sondheimer, F. *J. Am. Chem. Soc.* **1974**, 96, 5604.

(19) Wong, H. N. C.; Sondheimer, F. *Tetrahedron* **1981**, 37(S1), 99.

(20) de Graff, R. A. G.; Gorter, S.; Romers, C.; Wong, H. N. C.; Sondheimer, F. *J. Chem. Soc., Perkin Trans. 2* **1981**, 478.

(21) Chan, T.-L.; Mak, T. C. W.; Poon, C.-D.; Wong, H. N. C.; Jia, J. H.; Wang, L. L. *Tetrahedron* **1986**, 42, 655.

(22) Sheiner, A. C.; Schaefer, H. F., III *Chem. Phys. Lett.* **1991**, 177, 471.

(23) Leopold, D. G.; Stevens-Miller, A. E.; Lineberger, W. C. *J. Am. Chem. Soc.* **1986**, 108, 1379.

(24) Ervin, K. M.; Lineberger, W. C. In *Advances in Gas Phase Ion Chemistry*; Adams, N. G., Babcock, L. M., Eds.; JAI Press: Greenwich, 1992; Vol. 1, p 121.

(25) Lee, J.; Grabowski, J. *J. Chem. Rev.* **1992**, 92, 1611.

(26) Neumark, D. M.; Lykke, K. R.; Andersen, T.; Lineberger, W. C. *Phys. Rev. A* **1985**, 32, 1890.

(27) Moore, C. E. *Atomic Energy Levels*; US GPO: Washington, 1952; Circular No. 467.

(28) *Gaussian 94*, Frisch, M. J.; Trucks, G. W.; Schlegel, H. B.; Gill, P. M. W.; Johnson, B. G.; Robb, M. A.; Cheeseman, J. R.; Kieth, T.; Petersson, G. A.; Montgomery, J. A.; Raghavachari, K.; Al-Laham, M. A.; Zakrewski, V. G.; Ortiz, J. V.; Foresman, J. B.; Cioslowski, J.; Stefanov, B. B.; Nanayakkara, A.; Challacombe, M.; Peng, C. Y.; Ayala, P. Y.; Chen, W.; Wong, M. W.; Andres, J. L.; Replogle, E. S.; Gomperts, R.; Martin, R. L.; Fox, D. J.; Binkley, J. S.; Defrees, D. J.; Baker, J.; Stewart, J. J. P.; Head-Gordon, M.; Gonzalez, C.; Pople, J. A., Gaussian, Inc.: Pittsburgh, PA, 1994.

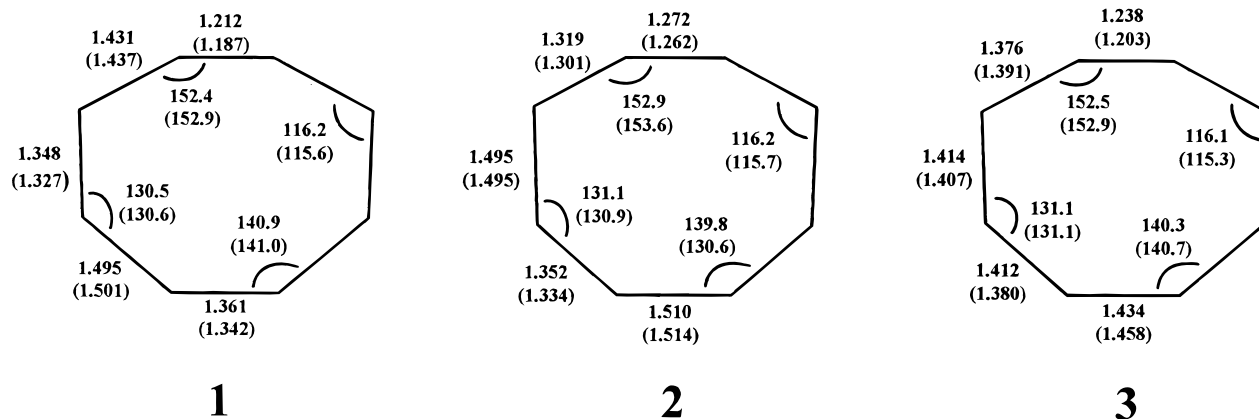


**Figure 1.** Calculated bond lengths and bond angles in **1**, **2**, and **3** at the Becke3LYP/6-31G\* and R(O)HF/6-31G\* (in parentheses) levels of theory. Bond lengths are in Å and bond angles are in deg.

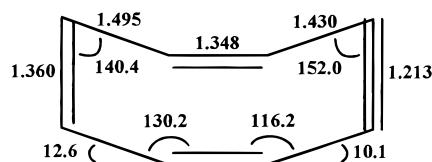


**Figure 2.** Calculated geometry of nonplanar **1**. This molecule is 0.01 kcal/mol lower in energy than the planar structure shown in Figure 1.

states. Most notable in all three structures is the very large CCC bond angle about the dehydrocarbons.

The energies of **1**, **2**, and **3** were calculated at the geometries shown in Figure 1. At the R(O)HF/6-31G\* and Becke3LYP/6-31G\* levels of theory, **1** is predicted to be the ground state, while **2** is calculated to be higher by 15.7 and 8.6 kcal/mol, respectively. However, the relative energies of cumulenenic and acetylenic systems are not calculated reliably with DFT methods, as allenic structures are favored by ~6 kcal/mol.<sup>29</sup> Therefore, **2** is likely higher in energy than **1** by *ca.* 14 kcal/mol, close to the RHF prediction. The <sup>3</sup>B<sub>2</sub> state, **3**, is calculated to be higher in energy than **1** by 18.3 and 7.8 kcal/mol at the R(O)HF/6-31G\* and Becke3LYP/6-31G\* levels of theory, respectively. Vibrational frequencies for **1**, **2**, and **3** were calculated with both the HF and DFT approaches. At the HF levels, all three states are calculated to be real minima; however, **1** is calculated to have one very low 19 cm<sup>-1</sup> vibrational frequency. At the Becke3LYP/6-31G\* level of theory, **2** and **3** do not contain any imaginary frequencies, but an imaginary mode of 36*i* was obtained for **1**, indicating that it is a saddle point. The normal coordinate corresponding to this mode is the one that transforms the planar molecule into a tub-like, C<sub>s</sub> symmetric structure similar to COT. The geometry of **1** was reoptimized in a separate calculation, without restricting to planarity. The optimized structure calculated at the Becke3LYP/6-31G\* level of theory is shown in Figure 2. A slightly nonplanar structure results, with all real vibrational frequencies but with an energy only 0.01 kcal/mol lower than that of planar **1**. This energy difference, the “ring-inversion” barrier in **1**, is much lower than the zero-point energy. Therefore, **1** is either a planar or “pseudoplanar” molecule, with a relatively flat potential energy surface. A shallow boat structure for **1** has been obtained previously by using MMX calculations.<sup>30</sup>

There are two electronic states of the dehydrocyclooctatetraene negative ion. A <sup>2</sup>A<sub>2</sub> state, **1**<sup>-</sup>, is formed by adding one electron into the a<sub>2</sub> orbital in **1**, while a <sup>2</sup>B<sub>1</sub> state, **2**<sup>-</sup>, is formed

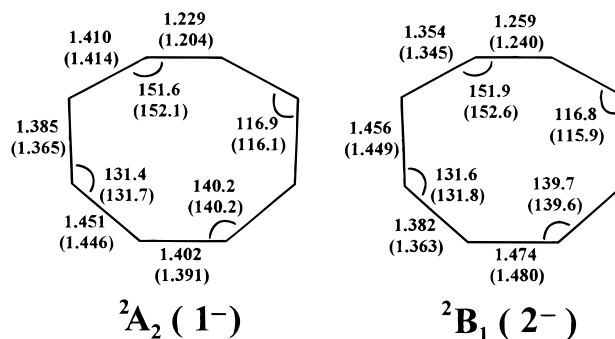


**Figure 3.** Structures of the <sup>2</sup>A<sub>2</sub> (**1**<sup>-</sup>) and <sup>2</sup>B<sub>1</sub> (**2**<sup>-</sup>) states of the DHCOT anion calculated at the Becke3LYP/6-31G\* and ROHF/6-31G\* (in parentheses) levels of theory. Bond lengths are in Å and bond angles are in deg.

by adding an electron to the b<sub>1</sub> orbital in **2**. These ions are expected to have geometries similar to the neutrals from which they are derived, except to have slightly longer double bonds and shorter single bonds because the extra electron occupies an antibonding π orbital. The geometries calculated for the two states of the ions at the Becke3LYP/6-31G\* and ROHF/6-31G\* levels of theory, shown in Figure 3, conform to these expectations. At these levels of theory, both states are predicted to be minima, and the <sup>2</sup>A<sub>2</sub> state of the ion is predicted to be lower in energy than the <sup>2</sup>B<sub>1</sub> state by 4.0 and 7.1 kcal/mol, respectively. The ESR spectrum of **1**<sup>-</sup>, reported by Stevenson and co-workers,<sup>31</sup> indicates that **1**<sup>-</sup> is a planar, π-type ion as described above, but does not differentiate between the two possible electronic states.

**Photoelectron Spectrum of 1<sup>-</sup>.** The photoelectron spectrum of the C<sub>8</sub>H<sub>6</sub><sup>-</sup> ion obtained from the reaction of O<sup>-</sup> with COT in a liquid nitrogen cooled flowing afterglow is shown in Figure 4. The major product of this reaction is expected to be the DHCOT ion that is obtained by removing hydrogens from adjacent carbons (1,2 abstraction).<sup>25</sup> Although the mass resolution of the Wien filter is not sufficient to separate the C<sub>8</sub>H<sub>6</sub><sup>-</sup> ions from other ions differing by only one or two mass units, the photoelectron spectrum shown in Figure 4 is very different from those obtained for authentic COT<sup>-</sup> and C<sub>8</sub>H<sub>7</sub><sup>-</sup> ions,<sup>8,32</sup> indicating that these ions are not formed to a significant extent under these conditions.

The structure of C<sub>8</sub>H<sub>6</sub><sup>-</sup> is assigned to the 1,2-DHCOT anion based on its reactivity.<sup>32</sup> The most important observation is

(31) Stevenson, G. R.; Colòn, M.; Concepción, J. G.; Block, A. M. *J. Am. Chem. Soc.* **1974**, *96*, 2283.

(32) Kato, S.; Lee, H. S.; Gareyev, R.; Wenthold, P. G.; Lineberger, W. C.; DePuy, C. H.; Bierbaum, V. M. *J. Am. Chem. Soc.* **1997**, *119*, 7863–7864.

(29) Plattner, D. A.; Houk, K. N. *J. Am. Chem. Soc.* **1995**, *117*, 4405.

(30) Yin, J.; Klosin, J.; Abdoud, K. A.; Jones, W. M. *Tetrahedron Lett.* **1995**, *36*, 3107.

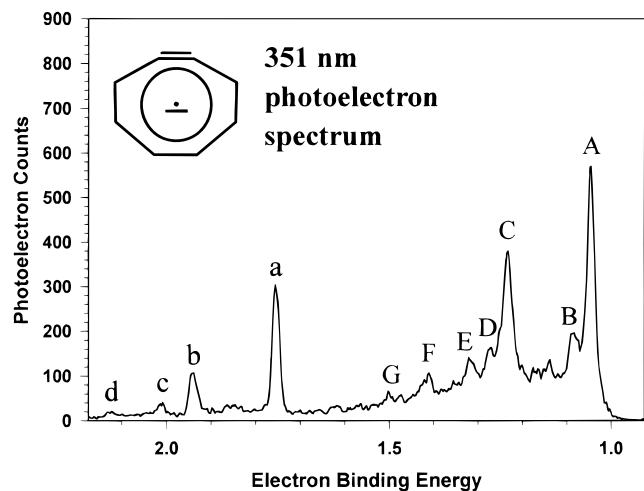


**Figure 4.** Photoelectron spectrum of **1<sup>-</sup>** prepared by the reaction of O<sup>-</sup> with cyclooctatetraene. The laser wavelength is 351 nm.

that the reaction of C<sub>8</sub>H<sub>6</sub><sup>-</sup> with NO leads to formation of cyanide ion, CN<sup>-</sup>, fairly rapidly. Ions formed by 1,3-, 1,4-, or 1,5-H<sub>2</sub><sup>+</sup> abstraction from COT would be open-shell ions, similar to the *m*- or *p*-benzyne ions, which react with NO to form adducts.<sup>33</sup> Adduct formation is not observed at all in the reaction of C<sub>8</sub>H<sub>6</sub><sup>-</sup> with NO, which indicates that the ion has a 1,2-DHCOT structure.

Two main features are observed in the photoelectron spectrum of the C<sub>8</sub>H<sub>6</sub><sup>-</sup> ion, and their relative intensities do not display a dependence on the source conditions. This indicates that the two features arise from detachment of the same state of the ion. If the two bands were due to different forms of C<sub>8</sub>H<sub>6</sub><sup>-</sup>, their relative intensities would be expected to be sensitive to source conditions, especially the source temperature. On the basis of these observations and the results of the density functional calculations described above, we conclude that essentially only one state of the ion is formed in the reaction of O<sup>-</sup> with COT, the <sup>2</sup>A<sub>2</sub> state of the 1,2-DHCOT anion, **1<sup>-</sup>**.

**State Assignments.** The features in the photoelectron spectrum can readily be assigned by using the results reported previously for COT<sup>-</sup>.<sup>8</sup> The lower energy state (peaks A–G) has an origin at a binding energy of 1.044 ± 0.008 eV. This value is very similar to the binding energy of 1.100 ± 0.006 eV obtained for the origin of the low energy state feature in the spectrum of COT<sup>-</sup>. For COT<sup>-</sup>, the low energy feature was assigned to formation of the planar, closed-shell singlet state of COT.<sup>8</sup> A similar assignment applies for the present system, where detachment of the electron from the singly occupied a<sub>2</sub> orbital in **1<sup>-</sup>** leads to formation of cyclooctatrienyne, **1**. Because **1** is the ground electronic state for this species, the measured binding energy for this state corresponds to the adiabatic electron affinity of **1**. Extensive vibrational activity is also observed for this state; however, the analysis will be addressed in a later section.

A second electronic state (peaks a–d) is observed in the photoelectron spectrum of **1<sup>-</sup>**, 0.708 ± 0.006 eV (16.3 ± 0.1 kcal/mol) above ground state. In the spectrum of COT<sup>-</sup>, a similar higher energy feature was observed and assigned to the triplet state. In the present study, the higher energy feature could be due to detachment to form the triplet, but could also result from detachment to form **2**. However, detachment of **1<sup>-</sup>** to form **2** is a two-electron transition, and would be expected to have a very weak cross section. Moreover, the Franck–Condon overlap between the alkyne-like structure of **1<sup>-</sup>** and the

**Table 1.** Peak Positions and Assignments for the Photoelectron Spectrum of **1<sup>-</sup>**

peak <sup>a</sup>	distance from origin, cm <sup>-1</sup>	calcd energy, <sup>b</sup> cm <sup>-1</sup>	peak height		assignt <sup>d</sup>
			rel <sup>c</sup>	calcd <sup>b</sup>	
Singlet (2)					
A	0	0	1.00	1.00	0 <sub>0</sub> <sup>0</sup>
B	290	295	0.37	0.46	1 <sub>0</sub> <sup>1</sup>
C	1500	1500	0.73	0.64	2 <sub>0</sub> <sup>1</sup>
D	1800	1795	0.33	0.30	1 <sub>0</sub> 2 <sub>0</sub> <sup>1</sup>
E	2185	2185	0.26	0.24	3 <sub>0</sub> <sup>1</sup>
F	2950	3000	0.19	0.21	2 <sub>0</sub> <sup>2</sup>
G	3670	3685	0.11	0.15	2 <sub>0</sub> 3 <sub>0</sub> <sup>1</sup>
Triplet (3)					
a	0	0	1.00	1.00	0 <sub>0</sub> <sup>0</sup>
b	1490	1490	0.30	0.35	2 <sub>0</sub> <sup>1</sup>
c	2060	2060	0.12	0.16	3 <sub>0</sub> <sup>1</sup>
d	2985	2980	0.06	0.06	2 <sub>0</sub> <sup>2</sup>

<sup>a</sup> Peaks labeled in Figure 4. <sup>b</sup> Peak positions and heights calculated by using the fitting procedure described in ref 24. <sup>c</sup> Experimental peak intensities for each state, relative to the origin. <sup>d</sup> Vibrational assignments are as follows: 1, ring-deformation; 2, bond alternation; 3, dehydrocarbon stretching. See text for details.

cumulene structure of **2** is calculated to be poor, with very little intensity in the origin.<sup>34–36</sup> The transition observed in the spectrum is strong and nearly vertical, which indicates that it is a one-electron process with a small geometry difference between the ion and the neutral, consistent with what one would expect for detachment of **1<sup>-</sup>** to give the triplet state, **3**. Therefore, the higher energy state is assigned to formation of **3**.

**Angular distribution measurements.** The photoelectron spectrum shown in Figure 4 was obtained with the electric field vector of the laser polarized at the “magic angle” (54.7°) with respect to the detector. The angular dependence of the photoelectron signal is described by eq 4,

$$I(\theta) = \left[ \frac{\sigma_{\text{tot}}}{4\pi} \right] \left[ 1 + \frac{\beta(3 \cos^2 \theta - 1)}{2} \right] \quad (4)$$

where  $\theta$  is the angle between the laser electric field and the detector,  $\sigma_{\text{tot}}$  is the total photodetachment cross section, and  $\beta$  is the anisotropy parameter ( $-1 \leq \beta \leq 2$ ).<sup>37–40</sup> At the magic angle, the photodetachment signal is independent of  $\beta$ .

The anisotropy parameters ( $\beta$ ) obtained for the features observed in the spectrum of **1<sup>-</sup>** are  $-0.62 \pm 0.10$  for the <sup>1</sup>A<sub>1</sub> ground state and  $-0.49 \pm 0.10$  for the <sup>3</sup>B<sub>2</sub> state. These are comparable to the values of  $-0.69 \pm 0.10$  and  $-0.58 \pm 0.10$  obtained for the corresponding transitions in the spectrum of COT<sup>-</sup>. This indicates that the electronic structure of **1<sup>-</sup>** is similar to that of COT<sup>-</sup>, as described above.

**Vibrational and Franck–Condon Analysis.** Extensive vibrational structure is observed for both of the observed electronic states in the spectrum of **1<sup>-</sup>**. The positions of all the observed peaks are listed in Table 1. For **1**, vibrational

(34) Franck–Condon factors calculated from calculated geometries and vibrational force fields. We thank Peter Chen and Cameron Logan for providing us with a copy of their CDECK program.

(35) Chen, P. In *Unimolecular and Bimolecular Reaction Dynamics*; Ng, C. Y., Baer, T., Powis, I., Eds.; John Wiley & Sons: New York, 1994.

(36) Wenthold, P. G.; Polak, M. L.; Lineberger, W. C. *J. Phys. Chem.* **1996**, *100*, 6920.

(37) Cooper, J.; Zare, R. N. *J. Chem. Phys.* **1968**, *48*, 942.

(38) Cooper, J.; Zare, R. N. *J. Chem. Phys.* **1968**, *49*, 4252.

(39) Hall, J. L.; Siegel, M. W. *J. Chem. Phys.* **1968**, *48*, 943.

(40) Hanstorp, D.; Bengtsson, C.; Larson, D. J. *Phys. Rev. A* **1989**, *40*, 670.

(33) Wenthold, P. G.; Hu, J.; Squires, R. R. *J. Am. Chem. Soc.* **1996**, *118*, 11865.

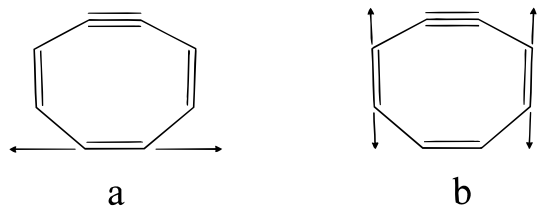


**Figure 5.** Calculated normal modes that comprise the “bond alternation” coordinate in **1**.

frequencies of  $295 \pm 20$ ,  $1500 \pm 20$ , and  $2185 \pm 20$   $\text{cm}^{-1}$  are obtained. The vibrational frequency of  $2185$   $\text{cm}^{-1}$  is readily assigned to the  $\text{C}\equiv\text{C}$  stretching mode. This value is similar to those that have been observed previously in cyclic alkynes,<sup>1</sup> but is significantly higher than the value of  $1860$   $\text{cm}^{-1}$  found for *o*-benzyne.<sup>23</sup> As expected, the DFT values for this frequency for the planar and nonplanar states of **1**,  $2320$  and  $2315$   $\text{cm}^{-1}$ , respectively, are slightly higher than the measured value.

The  $1500$   $\text{cm}^{-1}$  vibrational frequency is midway between the values of  $1315$  and  $1670$   $\text{cm}^{-1}$  observed previously for planar COT. Those frequencies were assigned to the “bond alternation” mode of  $D_{4h}$  COT,<sup>8</sup> in which the short carbon-carbon bonds are lengthened while the long bonds are shortened. The  $1500$   $\text{cm}^{-1}$  frequency found for **1** corresponds, in principle, to the same type of bond alternation mode. However, for **1** this coordinate is split into two separate carbon-carbon stretching components, as shown in Figure 5. The mode shown in Figure 5a corresponds to stretching of the carbon-carbon double bond opposite the dehydro carbons, and the mode in Figure 5b is primarily stretching of the double bonds adjacent to the dehydrocarbons. The frequencies for these modes are calculated to be  $1655$  and  $1688$   $\text{cm}^{-1}$ , respectively, for the planar form of **1**, and  $1665$  and  $1684$   $\text{cm}^{-1}$ , respectively, for nonplanar **1**. The calculation suggests that both modes may be active in the photoelectron spectrum but would not be resolved. In fact, we observe a weak shoulder on the high energy side of the peak near  $1.23$  eV, which might be due to a second bond stretching mode.

In  $D_{4h}$  COT, the first excited vibrational level of the bond alternation mode lies near the barrier for isomerization in a symmetric double-well potential such that the energy levels are split.<sup>8</sup> This splitting is observed in the photoelectron spectrum of  $\text{COT}^-$  to be  $355$   $\text{cm}^{-1}$ .<sup>8</sup> In the spectrum of **1**<sup>-</sup>, we observe only a single vibrational peak for this mode because the excited vibrational states of **1** are well below the barrier for isomerization to **2**. Schematic potential energy surfaces for bond alternation in COT and DHCOT are shown in Figure 6. Unlike that for planar COT,<sup>8</sup> the surface for DHCOT does not contain a symmetric double-well potential, as the two wells correspond to **1** and **2**, which are calculated to have significantly different energies.

A third vibrational peak for **1** is observed at  $295$   $\text{cm}^{-1}$  and is assigned to a ring deformation mode, qualitatively similar to  $\nu_{6a}$  in benzene (using Wilson numbering<sup>41</sup>). This mode is found to be active in most photoelectron spectra of ions that contain an aromatic system,<sup>23,42-44</sup> but was not observed in the spectrum of  $\text{COT}^-$ .<sup>8</sup>

For the triplet state, two distinct vibrational progressions are observed. The first corresponds to a vibrational frequency of

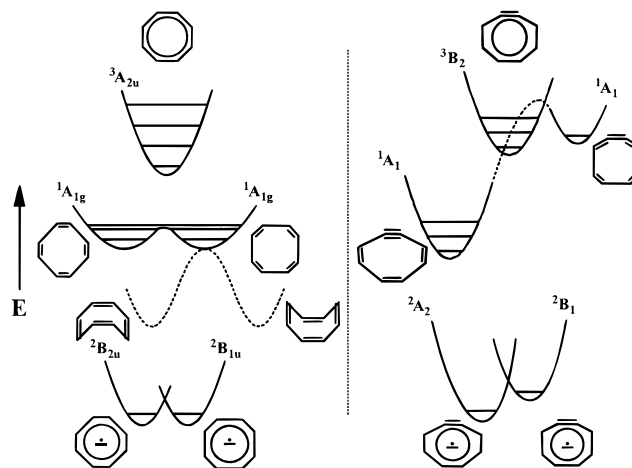


**Figure 6.** Schematic potential energy surfaces for the anionic and neutral states of COT (left) and DHCOT (right). The *x*-axis is the “bond-alternation” coordinate for the planar molecule. The height of the energy barrier between **1** and **2**, shown as a dashed curve on the right half of the figure, is not known. The dashed curve on the COT surface indicates the energy for out-of-plane bending of the  $D_{4h}$   $^1A_{1g}$  state.

$1490 \pm 20$   $\text{cm}^{-1}$ , and is assigned to the same type of bond alternation coordinate as for **1** (Figure 6). Unlike what was found with **1**, where bond alternation was calculated to be comprised of two nearly degenerate stretching components, a single stretching frequency is predicted for **3**, at  $1570$   $\text{cm}^{-1}$ . A second vibrational frequency is observed for **3**, at  $2060 \pm 20$   $\text{cm}^{-1}$ , which is the dehydrocarbon C-C stretching mode. The vibrational frequency for this mode is slightly lower than that for **1**, consistent with weakening of the triple bond. In fact, the calculated frequency for this mode ( $2173$   $\text{cm}^{-1}$ ) agrees almost perfectly with that calculated for **2** ( $2166$   $\text{cm}^{-1}$ ), where only a double bond exists between the two dehydrocarbons. This reflects the nonbonding character of the  $\pi$  system in the triplet configuration.

For both states, there is weak, unresolved signal around  $700$ – $1000$   $\text{cm}^{-1}$  above the origin. This is approximately the same region where the “ring-breathing” mode was observed in the planar states of COT.<sup>8</sup> However, the signal observed in the photoelectron spectrum of **1**<sup>-</sup> does not correspond to a single transition and likely contains contributions from multiple modes.

The intensities of the vibrational peaks in the spectrum are determined by the Franck-Condon factors (FCFs) for the transition. The FCFs, the elements of the Duschinsky **K** matrix,<sup>45</sup> depend on the geometry differences between ion and neutral in a given normal coordinate, and are obtained by fitting the data with a modeling procedure described elsewhere.<sup>24</sup> For the low-energy state, **1**, the observed modes and the corresponding FCFs are as follows:  $295$  ( $0.260$   $\text{amu}^{1/2}$   $\text{\AA}$ ),  $1500$  ( $0.174$   $\text{amu}^{1/2}$   $\text{\AA}$ ), and  $2185$   $\text{cm}^{-1}$  ( $0.088$   $\text{amu}^{1/2}$   $\text{\AA}$ ). The peak positions and relative intensities calculated with these parameters are listed in Table 1. The observed vibrational modes and FCFs for the excited state, **3**, are  $1490$  ( $0.130$   $\text{amu}^{1/2}$   $\text{\AA}$ ) and  $2060$   $\text{cm}^{-1}$  ( $0.076$   $\text{amu}^{1/2}$   $\text{\AA}$ ). The normal coordinate displacements for the bond alternation mode are relatively large, consistent with the schematic potential energy surfaces shown in Figure 6. The dehydrocarbon stretching mode is weakly active for both states. This is in sharp contrast to what is observed for the singlet state of *o*-benzyne, where the normal coordinate displacement for the  $\text{C}\equiv\text{C}$  stretching mode is large ( $0.236$   $\text{amu}^{1/2}$   $\text{\AA}$ ).<sup>23</sup> However, this is due to the difference in the electronic structures of the two ions. The DHCOT negative ion is a  $\pi$

(41) Wilson, E. B., Jr. *Phys. Rev.* **1934**, *45*, 706.

(42) Gunion, R. F.; Gilles, M. K.; Polak, M. L.; Lineberger, W. C. *Int. J. Mass Spectrom. Ion Processes* **1992**, *117*, 601.

(43) Gunion, R. F.; Karney, W.; Wenthold, P. G.; Borden, W. T.; Lineberger, W. C. *J. Am. Chem. Soc.* **1996**, *118*, 5074.

(44) Wenthold, P. G.; Kim, J. B.; Lineberger, W. C. *J. Am. Chem. Soc.* **1996**, *119*, 1354.

(45) Duschinsky, F. *Acta Physicochim. URSS* **1937**, *7*, 551.

anion, and the triple bond is not significantly affected in the ion. On the other hand, the negative ion of *o*-benzyne is formed by adding an extra electron to the antibonding orbital of the triple bond.<sup>23</sup> Therefore, the bond between the dehydrocarbons is much weaker and longer in the anion than it is in the neutral,<sup>46</sup> which leads to poorer Franck–Condon factors for detachment.

**Comparison with COT.** It is instructive to compare the photoelectron spectrum of  $1^-$  with that reported previously for  $COT^-$ . In most respects, the spectra for the two ions are similar. For example, detachment to form the planar singlet and triplet states of the neutral is observed in both spectra, and the electron affinities and singlet–triplet splittings are similar. Moreover, the vibrational modes active in the spectrum of  $COT^-$  are also active in the spectrum of  $1^-$ . However, there are some important differences between the two systems. One is the aforementioned lack of splitting of the vibrational wave function in **1**. Second, the presence of the dehydrocarbons in **1** and **3** is detected in the photoelectron spectrum as an active C–C stretching vibration. Therefore, the 2060 and 2185  $cm^{-1}$  frequencies are observed in the spectrum of  $1^-$ , but not in the spectrum of  $COT^-$ . A third difference is observed in the relative energies of the singlet and triplet features. In planar COT, the  $^3A_{2u}$  state was found to be  $12.1 \pm 0.3$  kcal/mol higher in energy than the  $D_{4h}$   $^1A_{1g}$  state. For DHCOT, the energy difference between the singlet and triplet states is found to be  $16.3 \pm 0.1$  kcal/mol,  $\sim 4$  kcal/mol larger than that in COT. The origin of this increase

is most likely destabilization of the triplet state of DHCOT, which is not able to adopt its optimal geometry where the carbon–carbon bond lengths are all equal.

A more subtle but important difference is observed in the peak widths in each spectrum. For COT, the peak corresponding to formation of the planar singlet state is asymmetric and broad,<sup>8</sup> with a full-width at half-maximum (fwhm) of *ca.* 50 meV. This is much broader than the peaks corresponding to formation of the triplet state, which have fwhm  $\approx 20$  meV. The broadening of the singlet peak can be thought to be the result of dynamical and/or lifetime broadening due to the fact that the neutral is a transition state.<sup>47</sup> In contrast, the peaks corresponding to formation of the singlet and triplet states of DHCOT are identical, with fwhm  $\approx 20$  meV, and broadening of the singlet is not observed. This indicates that both states are real minima on the potential energy surface, and that they are planar or pseudoplanar molecules.

**Acknowledgment.** This work was supported by the National Science Foundation (Grant Nos. CHE 97-03486 and PHY 95-12150). We thank Dr. Shuji Kato and Professor Chuck DePuy for helpful discussion.

JA970934W

(46) Nash, J. J.; Squires, R. R. *J. Am. Chem. Soc.* **1996**, *118*, 11872 and references therein.

(47) Neumark, D. M. *Acc. Chem. Res.* **1993**, *26*, 153.